Rotational Resonances and Regge-like Trajectories in Lightly Doped Antiferromagnets

A. Bohrdt,[1,2,3,4,*] E. Demler,[4] and F. Grusdt[5,2]

[1]*Department of Physics and Institute for Advanced Study, Technical University of Munich, 85748 Garching, Germany*
[2]*Munich Center for Quantum Science and Technology (MCQST), Schellingstr. 4, D-80799 München, Germany*
[3]*ITAMP, Harvard-Smithsonian Center for Astrophysics, Cambridge, Massachusetts 02138, USA*
[4]*Department of Physics, Harvard University, Cambridge, Massachusetts 02138, USA*
[5]*Department of Physics and Arnold Sommerfeld Center for Theoretical Physics (ASC), Ludwig-Maximilians-Universität München, Theresienstr. 37, München D-80333, Germany*

(Received 2 March 2021; accepted 13 October 2021; published 5 November 2021)

Understanding the nature of charge carriers in doped Mott insulators holds the key to unravelling puzzling properties of strongly correlated electron systems, including cuprate superconductors. Several theoretical models suggested that dopants can be understood as bound states of partons, the analogues of quarks in high-energy physics. However, direct signatures of spinon-chargon bound states are lacking, both in experiment and theory. Here we propose a rotational variant of angle-resolved photo-emission spectroscopy (ARPES) and calculate rotational spectra numerically using the density-matrix renormalization group. We identify long-lived rotational resonances for an individual dopant, which we interpret as a direct indicator of the microscopic structure of spinon-chargon bound states. Similar to Regge trajectories reflecting the quark structure of mesons, we establish a linear dependence of the rotational energy on the superexchange coupling. The rotational peaks we find are strongly suppressed in standard ARPES spectra, but we suggest a multiphoton extension of ARPES which allows us to access rotational spectra. Our findings suggest that multiphoton spectroscopy experiments should provide new insights into emergent universal features of strongly correlated electron systems.

DOI: 10.1103/PhysRevLett.127.197004

Introduction.—Our understanding of strongly correlated quantum matter often involves new emergent structures. For example, emergent gauge fields play a central role for understanding quantum spin liquids [1], and spin-charge separation in the one-dimensional Hubbard model can be related to the fractionalization of fermions into deconfined spinons and chargons [2–4]. The fate of those partons in dimensions higher than 1, which is a topic addressed in this Letter, remains unresolved. Theoretically and experimentally, one faces similar problems as in high-energy physics: the mathematical models are too challenging to solve and signatures of parton formation are often indirect or buried in complex observables. In this Letter we draw analogies to high energy physics and report on unambiguous signatures for parton structures in the two-dimensional (2D) $t-J$ model.

In quantum chromodynamics it is well established that directly observable nucleons are not the most elementary constituents of matter. The quark model explains the larger class of mesons and baryons as composite objects consisting of two or three valence quarks. A smoking gun demonstration of the quark model was its ability to explain many additional resonances observed in collider experiments as rovibrational excitations of the fundamental parton configurations. In the quark model, many heavy mesons are thus understood as excited states of the fundamental mesons: they contain the same quark content but realize a higher vibrational state or have nonzero orbital angular momentum [5,6]. A hallmark signature of rotational mesons comes from analysis of their excitation energy. In a simplistic model, a meson can be described as a rigid linelike object with constant energy density per unit length, also known as "string tension." The relativistic expression for the energy of a rotating meson of this type scales linearly with the string tension and with the square root of its angular momentum [7]. The latter relation, known as the Regge trajectory, can be directly probed in collider experiments and has been observed experimentally [8]. It provides a strong indication that the observed mesons are bound states of partons.

An idea almost as old as the problem of high-T_c superconductivity itself comprises that strongly correlated electrons in these systems may be ruled by similar principles as high-energy physics [9]. In analogy with quark confinement, Béran *et al.* suggested a description of a hole doped into a 2D antiferromagnet (AFM) in terms of a composite quasiparticle, consisting of two partons—a chargon, carrying the charge quantum number and a spinon, carrying the spin quantum number—bound together by "an interaction obeying a string law" [10]. However, finding direct experimental or theoretical signatures for such structure has proven to be difficult. In angle resolved photoemission spectra (ARPES) no sign of rotational resonances has been seen, and the nature of a possible first vibrational excitation is debated [11–15].

Discerning the nature of individual charge carriers in lightly doped Mott insulators could provide a major boost to understanding properties of the underdoped cuprates and elucidating the origin of the pseudogap (PG) phase. In particular, it should provide a basis for constructing a consistent description of transport [17] and spectroscopy [18] experiments. Several theoretical proposals involve emergent structures of partons, starting on a single dopant level [10,14,19,20], to effective theories of the PG phase involving dynamical gauge fields [21–24], exotic composite Fermi liquids [25–27], scenarios with spin-charge separation [28,29], and including fractionalized Fermi liquids [30] where deconfined spinons and chargons form electronlike bound states [31–33]. These scenarios may also explain the sudden and pronounced change of ARPES spectra [34] and the carrier density [17] observed in cuprates around $p^* = 19\%$ doping, as being related to an unbinding transition of spinons and chargons.

Here we provide strong numerical evidence that individual charge carriers in a lightly doped 2D AFM Mott insulators are comprised of partons, which are bound to each other, and exhibit telltale rotational excitations following Regge-like trajectories. We show that these rotational excitations are strongly suppressed in standard ARPES measurements and propose an extension of ARPES imparting C_4-angular momentum into the system and allowing us to access rotational excitations experimentally in solids [35] or using ultracold atoms [36,37]. Our numerical density-matrix renormalization group (DMRG) simulations of the one-hole rotational ARPES spectra in the $t-J$ model, see Fig. 1, reveal narrow quasiparticle peaks at low excitation energies, which we interpret as a striking proof of the parton picture. Moreover, we describe the rotational resonances by a microscopic spinon-chargon toy model which explains the observed features without any free fit parameters.

Rotational ARPES spectrum.—In traditional ARPES the spectral function $A(\boldsymbol{k},\omega) = -\pi^{-1}\mathrm{Im}\mathcal{G}(\boldsymbol{k},\omega)$ is measured, which reveals information about the one-hole Green's function $\mathcal{G}(\boldsymbol{j},t) = \theta(t)\sum_\sigma \langle \Psi_0|\hat{c}^\dagger_{\boldsymbol{j},\sigma}(t)\hat{c}_{\boldsymbol{0},\sigma}(0)|\Psi_0\rangle$; the latter describes how a fermion $\hat{c}_{\boldsymbol{j},\sigma}$ with spin σ is removed from the initial state $|\Psi_0\rangle$ and leads to a hole propagating through the system. In the 2D Fermi-Hubbard model, believed to describe lightly doped copper oxides [9], a long-lived quasiparticle peak is found in $A(\boldsymbol{k},\omega)$ [38–40], which describes how a hole interacting with magnetic fluctuations forms a spin or magnetic polaron [11,41–45] and moves through the surrounding AFM.

Our goal is to search for long-lived rotational excitations in the one-hole spectrum, which provide a direct route to reveal the composite nature of charge carriers in the Hubbard or $t-J$ models. To couple to rotationally excited states one must impart discrete C_4 angular momentum into the system. However, Green's function $\mathcal{G}(\boldsymbol{k},\omega)$ respects the symmetries of the underlying Hamiltonian: In this case we are particularly interested in the discrete rotational C_4 symmetry of the

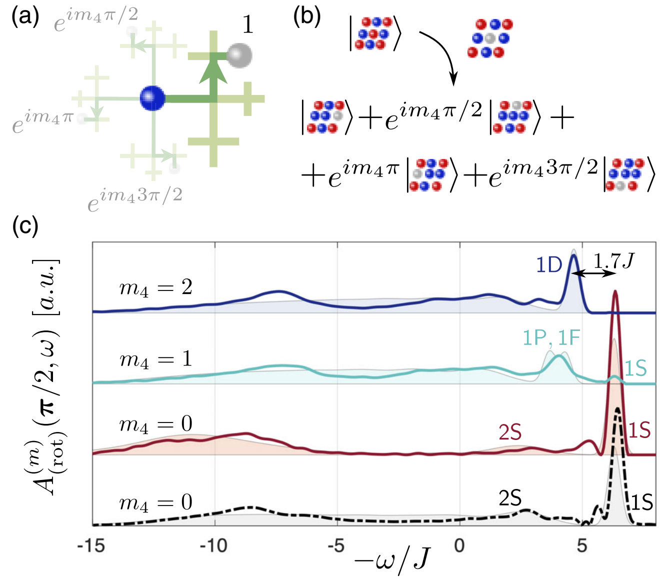

FIG. 1. Rotational resonances. (a) Bound states of spinons and chargons in a C_4-symmetric doped 2D AFM Mott insulators feature characteristic rovibrational excitations. In an effective microscopic theory, the string with the light chargon (gray) can rotate around the heavy spinon (blue). (b) To detect rotational resonances, we propose a multiphoton ARPES scheme. Following the creation of a hole by a first photon, a second photon couples to lattice vibrations and excites rotational modes with C_4 angular momentum $m_4 = 0$, 1, 2, 3. (c) Energy distribution curves for rotational ARPES spectra at the nodal point $\boldsymbol{k} = \boldsymbol{\pi}/2$ with different angular momenta, from top to bottom: $m_4 = 2$, 1, 0. The lowest (dash-dotted) curve corresponds to the usual ARPES spectrum with $m_4 = 0$. All spectra are normalized by their total area, $\int d\omega A^{(m)}_{(\mathrm{rot})}$. The lowest mesonic resonances (ground state 1S, vibrational 2S and rotational 1P, 1D, 1F excited states) correspond to long-lived excited states. We performed time-dependent DMRG simulations for a $t-J$ model on a 4×40 cylinder, with $t = 3J$. The shaded areas correspond to toy model calculations [16] where we introduced small energy shifts and broadening as fit parameters.

Hubbard model, which is unbroken in the undoped parent AFM $|\Psi_0\rangle$. Hence, for C_4 invariant momenta (C4IM) in the magnetic Brillouin zone (MBZ) no angular momentum transfer is allowed and rotational excitations have no weight in the traditional ARPES spectrum $A(\boldsymbol{k},\omega)$.

For non-C4IM, lattice effects can, in principle, impart C_4 angular momentum into the system. However, since Green's function couples to the center-of-mass momentum $\boldsymbol{k}$ of the hole, the spectral weight of rotational states is still expected to be strongly suppressed if the effective masses of the two supposed partons are significantly different. In this limit, the lighter parton rotates around the heavier parton which carries most of the linear momentum $\boldsymbol{k}$, thus suppressing couplings of $\boldsymbol{k}$ to the *relative* angular momentum of the two partons; this intuition is confirmed for toy models [16]. The Hubbard model in cuprates, with superexchange coupling $J \approx t/3$, is in such a regime where significantly different parton masses $\simeq 1/J$ and $\simeq 1/t$ are expected.

To allow significant overlap with possible rotational excitations, we devise a rotational extension of ARPES where angular momentum is directly imparted into the system, even at C4IM. The simplest term creating an excitation with discrete angular momentum $m_4 = 0$, 1, 2, 3, spin σ, charge one, and total momentum $\boldsymbol{k}$ is given by

$$\hat{R}_{m_4,\sigma}(\boldsymbol{k}) = \sum_{\boldsymbol{j}} \frac{e^{-i\boldsymbol{k}\cdot\boldsymbol{j}}}{\sqrt{V}} \sum_{\boldsymbol{i}:\langle \boldsymbol{i},\boldsymbol{j}\rangle} e^{im_4\varphi_{\boldsymbol{i}-\boldsymbol{j}}} \sum_{\sigma'} \hat{c}^{\dagger}_{\boldsymbol{j},\sigma'} \hat{c}_{\boldsymbol{i},\sigma'} \hat{c}_{\boldsymbol{j},\sigma}, \quad (1)$$

with $\varphi_{\boldsymbol{r}} = \arg(\boldsymbol{r})$ the polar angle of $\boldsymbol{r}$. The action of this operator on a product Néel state, $\hat{R}_{m_4,\sigma}|\mathrm{N}\rangle$, is illustrated in Fig. 1(b): Here the second and third fermion operators in $\hat{R}_{m_4,\sigma}$ create a stringlike excitation with C_4 angular momentum m_4 and nonzero overlap to the rotational states predicted for a hole in an Ising AFM [46].

Instead of the usual Green's function, we consider the rotational Green's function

$$\mathcal{G}^{(m_4)}_{\mathrm{rot}}(\boldsymbol{k},t) = \theta(t) \sum_{\sigma} \langle \Psi_0 | \hat{R}^{\dagger}_{m_4,\sigma}(\boldsymbol{k},t) \hat{R}_{m_4,\sigma}(\boldsymbol{k},0) | \Psi_0 \rangle, \quad (2)$$

which we calculate by time-dependent DMRG (see Ref. [47]) [48–50]. The corresponding rotational spectrum, $-\pi^{-1}\mathrm{Im}\mathcal{G}^{(m_4)}_{\mathrm{rot}}(\boldsymbol{k},\omega)$, in Lehmann representation is

$$A^{(m_4)}_{\mathrm{rot}}(\boldsymbol{k},\omega) = \sum_{\sigma,n>0} \delta(\omega - E_n + E_0) |\langle \Psi_n | \hat{R}_{m_4,\sigma}(\boldsymbol{k}) | \Psi_0 \rangle|^2, \quad (3)$$

where $|\Psi_0\rangle$ (E_0) is the correlated ground state (energy) and $|\Psi_n\rangle$ (E_n) for $n > 0$ are the eigenstates (eigenenergies) with an added hole. Hence, if long-lived rotational excitations exist, they manifest in pronounced quasiparticle peaks in the rotational ARPES spectrum in Eq. (3). For $m_4 = 0$ the same selection rules apply as for the conventional ARPES spectrum and the same states contribute, but with modified spectral weights.

The rotational spectrum can be experimentally measured using a multiphoton extension of ARPES. We propose to use one set of beams for lattice modulation, which imparts angular momentum into the system by coupling to specific phonon modes [56] or directly by modulating the lattice potential with appropriate phases in solids or ultracold atoms [57]. The other beam is the usual ARPES beam which creates the hole excitation. Further details of our scheme are provided in Ref. [16].

Rotational resonances.—Now we present our numerical results obtained for one hole doped into a 2D AFM Mott insulator. Specifically, we considered the $t-J$ model on extended four-leg cylinders and for $t/J = 3$, the experimentally most relevant value for cuprates. In Fig. 1(c) we show numerically obtained spectra (energy distribution curves) at the nodal point $\boldsymbol{k} = \boldsymbol{\pi}/2$, with $\boldsymbol{\pi} = (\pi, \pi)$. For $m_4 = 0$ (red line, second from bottom) the rotational spectrum shows the same quasiparticle peak as the conventional ARPES spectrum (black, bottom line), at the same energy. This peak, labeled 1S, corresponds to the magnetic polaron ground state [15]. A possible excited state with small spectral weight is also visible at $m_4 = 0$, which we label 2S and which has previously been argued to correspond to the first vibrational excitation of the magnetic polaron [11–15].

Much clearer indications for long-lived excitations of magnetic polarons can be found in the nontrivial rotational ARPES spectra with $m_4 \neq 0$. For $m_4 = 2$ (top, blue curve in Fig. 1) we find a pronounced quasiparticle peak corresponding to an excitation energy $\Delta E \sim 1.7J$. Remarkably, no significant spectral weight appears below this energy; in particular, we find zero spectral weight at the polaron ground state energy. We note that this is not simply a consequence of selection rules: First, the nodal point does not correspond to a C4IM, not even in the reduced MBZ. Second, the AFM has gapless magnon modes which should in principle allow us to carry away angular momentum and allow an excited magnetic polaron to decay to its ground state. Based on these observations, we identify the resonance found at $m_4 = 2$ with a 1D excited state of the magnetic polaron.

Similarly, the rotational spectrum with $m_4 = 1$ features a pronounced peak at a slightly higher excitation energy $\Delta E \sim 2.3J$ above the ground state (second from top, turquoise curve in Fig. 1). In this case we find weak hybridization with the 1S state, as indicated by a small quasiparticle peak at the ground state energy. Based on its quantum numbers, we identify the new excited state as 1P. By applying a combination of time-reversal and inversion symmetry, it follows that the $m_4 = 1$ and $m_4 = 3$ rotational spectra coincide exactly. Hence the 1P state is associated with a degenerate 1F state at $m_4 = 3$.

Our observation of long-lived quasiparticle peaks in the rotational spectrum provides a direct indication that mobile holes in lightly doped AFM Mott insulators have a discrete internal structure. To understand our reasoning, consider a theoretical model of magnetic polarons without a rigid internal structure. In this case, the action of the operator $\hat{R}_{m_4,\sigma}(\boldsymbol{k})$ in the rotational Green's function would generically be expected to have two separate effects: The first fermion operator $\hat{c}_{\boldsymbol{j},\sigma}$ in Eq. (1) creates a mobile hole with a large overlap to the structureless magnetic polaron. The subsequent pair of fermion operators, $\sum_{\sigma'} \hat{c}^{\dagger}_{\boldsymbol{j},\sigma'} \hat{c}_{\boldsymbol{i},\sigma'}$ in Eq. (1), then couples to the surrounding spins and creates separate magnon excitations. In this case one would expect $A^{(m_4)}_{\mathrm{rot}}(\boldsymbol{k},\omega)$ to become a convolution of a polaron and a magnon contribution, possibly renormalized weakly by interaction effects. This would lead to a broad and mostly featureless spectrum—in stark contrast with our numerical findings in Fig. 1(c).

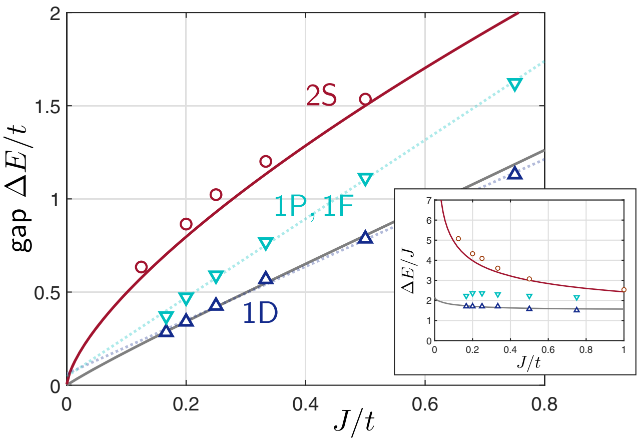

FIG. 2. Regge-like trajectories. We show the dependence of the excitation gap ΔE at the nodal point $\boldsymbol{k} = \boldsymbol{\pi}/2$ on the superexchange energy J. The gap was extracted from peak positions in numerically obtained spectra. The low-lying rotational resonances (1P, 1D, 1F) have a gap scaling linearly with J (light dotted lines denote linear fits: $\Delta E_{\mathrm{1D}} = 1.44J + 0.061t$ and $\Delta E_{\mathrm{1P,1F}} = 2.12J + 0.047t$). The gap to the first vibrational peak (2S) scales with $t^{1/3}J^{2/3}$ [15]. Solid lines are parameter-free calculations neglecting spinon dynamics [16]. The inset shows the same data, but with energy measured in units of J instead of t.

Regge-like trajectories.—Béran *et al.* [10] have suggested that mobile holes in an AFM Mott insulator can be described as mesonic bound states of two strongly interacting partons, a light chargon and a heavy spinon; see also Refs. [46,58]. The operators $\hat{R}_{m_4,\sigma}(\boldsymbol{k})$ create rotational excitations, which explains the peaks in the rotational spectra in Fig. 1. Now we study how the excitation energies ΔE of these rotational peaks, as well as the first vibrational peak, depend on the underlying coupling strength J/t in the system.

In Fig. 2 we numerically extracted the positions of the peaks from frequency cuts $A_{\mathrm{rot}}^{(m_4)}(\boldsymbol{\pi}/2, \omega)$ of rotational spectra at the nodal point, for different values of J/t. We find that the positions of the rotational peaks scale linearly with the spin exchange

$$\Delta E_{\mathrm{rot}} \simeq J, \tag{4}$$

whereas the gap to the vibrational excitation 2S has a characteristic power-law dependence on t and J [15],

$$\Delta E_{\mathrm{vib}} \simeq t^{1/3}J^{2/3}. \tag{5}$$

These scaling behaviors can be explained by a simplistic meson model [46]: In this model the two partons are connected by a line-like object on the square lattice with constant energy density $dE/d\ell$. This string tension must be proportional to the spin exchange energy $dE/d\ell \propto J$ to obtain the observed scaling laws in Eqs. (4) and (5).

Since J corresponds to the string tension between the two partons, Eq. (4) resembles the Regge formula from particle physics, which relates the meson excitation energy to its angular momentum and the underlying string tension [7]. While high-energy experiments cannot tune the string tension, which is determined by the coupling constant g of quantum chromodynamics, cold atom quantum simulators [37,45,59,60] can be used to tune the coupling J/t in the Hubbard model and directly measure the Regge-like trajectories we predict for rotational excitations in Fig. 2.

In further analogy with the Regge formula from high-energy physics, we can study the dependence of the meson excitation energy ΔE on its angular momentum m_4. While quarks in high-energy physics are described in a continuous space-time, lattice effects are strong in the Hubbard or $t-J$ models we consider. As a result, the simplistic meson model from Ref. [46] predicts that all rotational states with $m_4 \neq 0$ should be degenerate when $J/t \ll 1$, and be located between purely vibrational states in this limit. Refined meson models predict small splittings of the rotational lines, however. We confirm in Fig. 2 that all rotational excitations are close in energy, and well separated from the first vibrational peak.

Discussion and outlook.—We have proposed a rotational extension of ARPES, which we used to predict the previously unknown long-lived rotational excitations of individual charge carriers in 2D AFM Mott insulators. Our finding of pronounced quasiparticle peaks in the rotational spectra allows us to conclude that strong interactions between spin and charge must be present. By analyzing Regge-like trajectories, describing the dependence of the excitation energy on the superexchange J, we found compelling evidence that mobile holes in lightly doped AFM Mott insulators have a rich internal structure and can be understood as spinon-chargon bound states. This finding is further supported by the good agreement we report with a microscopic toy model of spinons and chargons connected by a string [16].

Our research provides the most direct evidence yet for the decades old idea [10,58] that the physics of lightly doped 2D AFM Mott insulators—and by extension high-temperature superconductors—is captured by emergent partons. In particular our results support the picture of the pseudogap phase in cuprates as a liquid of fermionic mesons, modeling charge carriers as bound states of spinons and chargons. We emphasize the importance of a direct experimental confirmation that charge carriers have a rich internal structure: An observation of the long-lived rotational resonances we predict would strongly support this view. Experiments, and further theoretical analysis, will be required to investigate the robustness of the internal structure of charge carriers when the concentration of dopants is increased.

The meson structure of charge carriers in lightly doped 2D AFM Mott insulators may have further theoretical implications. On the one hand it may contribute to our understanding how stripes form at low temperatures [61]. On the other hand, understanding possible unbinding transitions of spinons and chargons may contribute to a deeper understanding of the rich phase diagram of cuprates. An interesting future direction would be to explore how the parton picture relates to the sudden change of carrier properties observed around a critical doping $p^* \approx 19\%$ [17,34,62]; see also Ref. [63].

The authors thank M. Knap, Z. X. Shen, A. Cavalleri, E.-A. Kim, I. Morera Navarro, S. Sachdev, U. Schollwöck, I. Bloch, M. Greiner, J. Koepsell, and F. Pollmann for fruitful discussions. This research was supported by the Deutsche Forschungsgemeinschaft (DFG, German Research Foundation) under Germany's Excellence Strategy—EXC-2111–390814868. E. D. was supported by the ARO Grant No. W911NF-20-1-0163, the NSF Grant No. EAGER-QAC-QSA 2222-206-2014111, the NSF Grant No. OAC-1934714, and the Harvard-MIT CUA.

[*]Corresponding author.
annabelle.bohrdt@cfa.harvard.edu

[1] X.-G. Wen, *Quantum Field Theory of Many-body Systems* (Oxford University Press, New York, 2004).
[2] T. Giamarchi, *Quantum Physics in One Dimension* (Oxford University Press, New York, 2003).
[3] C. Kim, A. Y. Matsuura, Z.-X. Shen, N. Motoyama, H. Eisaki, S. Uchida, T. Tohyama, and S. Maekawa, Observation of Spin-Charge Separation in One-Dimensional $SrCuO_2$, Phys. Rev. Lett. **77**, 4054 (1996).
[4] J. Vijayan, P. Sompet, G. Salomon, J. Koepsell, S. Hirthe, A. Bohrdt, F. Grusdt, I. Bloch, and C. Gross, Time-resolved observation of spin-charge deconfinement in fermionic hubbard chains, Science **367**, 186 (2020).
[5] L. Micu, Decay rates of meson resonances in a quark model, Nucl. Phys. **B10**, 521 (1969).
[6] K. A. Olive *et al.* (Particle Data Group), Review of particle physics, Chin. Phys. C **38**, 090001 (2014).
[7] J. Greensite, The confinement problem in lattice gauge theory, Prog. Part. Nucl. Phys. **51**, 1 (2003).
[8] G. S. Bali, QCD forces and heavy quark bound states, Phys. Rep. **343**, 1 (2001).
[9] P. A. Lee, N. Nagaosa, and X.-G. Wen, Doping a mott insulator: Physics of high-temperature superconductivity, Rev. Mod. Phys. **78**, 17 (2006).
[10] P. Beran, D. Poilblanc, and R. B. Laughlin, Evidence for composite nature of quasiparticles in the 2d t-J model, Nucl. Phys. **B473**, 707 (1996).
[11] E. Dagotto, R. Joynt, A. Moreo, S. Bacci, and E. Gagliano, Strongly correlated electronic systems with one hole: Dynamical properties, Phys. Rev. B **41**, 9049 (1990).
[12] P. W. Leung and R. J. Gooding, Dynamical properties of the single-hole t-J model on a 32-site square lattice, Phys. Rev. B **52**, R15711 (1995).
[13] A. S. Mishchenko, N. V. Prokof'ev, and B. V. Svistunov, Single-hole spectral function and spin-charge separation in the $t - J$ model, Phys. Rev. B **64**, 033101 (2001).
[14] E. Manousakis, String excitations of a hole in a quantum antiferromagnet and photoelectron spectroscopy, Phys. Rev. B **75**, 035106 (2007).
[15] A. Bohrdt, E. Demler, F. Pollmann, M. Knap, and F. Grusdt, Parton theory of arpes spectra in anti-ferromagnetic mott insulators, Phys. Rev. B **102**, 035139 (2020).
[16] A. Bohrdt, E. Demler, and F. Grusdt, Rotational resonances and regge trajectories in lightly doped antiferromagnets, arXiv:2101.09280.
[17] S. Badoux, W. Tabis, F. Laliberte, G. Grissonnanche, B. Vignolle, D. Vignolles, J. Beard, D. A. Bonn, W. N. Hardy, R. Liang, N. Doiron-Leyraud, L. Taillefer, and C. Proust, Change of carrier density at the pseudogap critical point of a cuprate superconductor, Nature (London) **531**, 210 (2016).
[18] K. M. Shen, F. Ronning, D. H. Lu, F. Baumberger, N. J. C. Ingle, W. S. Lee, W. Meevasana, Y. Kohsaka, M. Azuma, M. Takano, H. Takagi, and Z.-X. Shen, Nodal quasiparticles and antinodal charge ordering in $ca_{2-x}na_xcuo_2cl$, Science **307**, 901 (2005).
[19] L. N. Bulaevskii, E. L. Nagaev, and D. I. Khomskii, A new type of auto-localized state of a conduction electron in an antiferromagnetic semiconductor, J. Exp. Theor. Phys. **27**, 836 (1968), http://www.jetp.ras.ru/cgi-bin/e/index/e/27/5/p836?a=list.
[20] S. A. Trugman, Interaction of holes in a hubbard antiferromagnet and high-temperature superconductivity, Phys. Rev. B **37**, 1597 (1988).
[21] G. Baskaran and P. W. Anderson, Gauge theory of high-temperature superconductors and strongly correlated fermi systems, Phys. Rev. B **37**, 580 (1988).
[22] A. Nakamura and T. Matsui, Ginzburg-landau theory of resonating valence bonds and its U(1) phase dynamics, Phys. Rev. B **37**, 7940 (1988).
[23] D. P. Arovas and A. Auerbach, Functional integral theories of low-dimensional quantum heisenberg models, Phys. Rev. B **38**, 316 (1988).
[24] I. Ichinose and T. Matsui, Dynamics of holes and spins in the hubbard t-J model and high-temperature superconductivity, Phys. Rev. B **45**, 9976 (1992).
[25] P. W. Anderson, "Luttinger-Liquid" Behavior of the Normal Metallic State of the 2d Hubbard Model, Phys. Rev. Lett. **64**, 1839 (1990).
[26] P. W. Anderson, Hidden Fermi liquid: The secret of high-T_c cuprates, Phys. Rev. B **78**, 174505 (2008).
[27] G. Baskaran, 3/2-fermi liquid: The secret of high-tc cuprates, arXiv:0709.0902.
[28] I. Ichinose, T. Matsui, and M. Onoda, Effective gauge-field theory of the $t - J$ model in the charge-spin separated state and its transport properties, Phys. Rev. B **64**, 104516 (2001).
[29] I. Ichinose and T. Matsui, Mechanism of charge-spin separation in the t-J model: Dynamics of u(1) gauge theory with multiple gauge fields, Phys. Rev. B **51**, 11860 (1995).
[30] T. Senthil, S. Sachdev, and M. Vojta, Fractionalized Fermi Liquids, Phys. Rev. Lett. **90**, 216403 (2003).
[31] M. Punk, A. Allais, and S. Sachdev, Quantum dimer model for the pseudogap metal, Proc. Natl. Acad. Sci. U.S.A. **112**, 9552 (2015).

[32] S. Sachdev and D. Chowdhury, The novel metallic states of the cuprates: Topological fermi liquids and strange metals, Prog. Theor. Exp. Phys. **2016**, 12C102 (2016).

[33] Y.-H. Zhang and S. Sachdev, From the pseudogap metal to the Fermi liquid using ancilla qubits, Phys. Rev. Research **2**, 023172 (2020).

[34] S.-D. Chen, M. Hashimoto, Y. He, D. Song, K.-. Xu, J.-F. He, T. P. Devereaux, H. Eisaki, D.-H. Lu, J. Zaanen, and Z.-X. Shen, Incoherent strange metal sharply bounded by a critical doping in bi2212, Science **366**, 1099 (2019).

[35] A. Damascelli, Z. Hussain, and Z.-X. Shen, Angle-resolved photoemission studies of the cuprate superconductors, Rev. Mod. Phys. **75**, 473 (2003).

[36] A. Bohrdt, D. Greif, E. Demler, M. Knap, and F. Grusdt, Angle-resolved photoemission spectroscopy with quantum gas microscopes, Phys. Rev. B **97**, 125117 (2018).

[37] P. T. Brown, E. Guardado-Sanchez, B. M. Spar, E. W. Huang, T. P. Devereaux, and W. S. Bakr, Angle-resolved photoemission spectroscopy of a fermi-hubbard system, Nat. Phys. **16**, 26 (2020).

[38] B. O. Wells, Z. X. Shen, A. Matsuura, D. M. King, M. A. Kastner, M. Greven, and R. J. Birgeneau, *e* Versus k Relations and Many Body Effects in the Model Insulating Copper Oxide $sr_2cuo_2cl_2$, Phys. Rev. Lett. **74**, 964 (1995).

[39] F. Ronning, K. M. Shen, N. P. Armitage, A. Damascelli, D. H. Lu, Z.-X. Shen, L. L. Miller, and C. Kim, Anomalous high-energy dispersion in angle-resolved photoemission spectra from the insulating cuprate $ca_2cuo_2cl_2$, Phys. Rev. B **71**, 094518 (2005).

[40] J. Graf, G.-H. Gweon, K. McElroy, S. Y. Zhou, C. Jozwiak, E. Rotenberg, A. Bill, T. Sasagawa, H. Eisaki, S. Uchida, H. Takagi, D.-H. Lee, and A. Lanzara, Universal High Energy Anomaly in the Angle-Resolved Photoemission Spectra of High Temperature Superconductors: Possible Evidence of Spinon and Holon Branches, Phys. Rev. Lett. **98**, 067004 (2007).

[41] C. L. Kane, P. A. Lee, and N. Read, Motion of a single hole in a quantum antiferromagnet, Phys. Rev. B **39**, 6880 (1989).

[42] S. Sachdev, Hole motion in a quantum néel state, Phys. Rev. B **39**, 12232 (1989).

[43] G. Martinez and P. Horsch, Spin polarons in the t-J model, Phys. Rev. B **44**, 317 (1991).

[44] Z. Liu and E. Manousakis, Dynamical properties of a hole in a heisenberg antiferromagnet, Phys. Rev. B **45**, 2425 (1992).

[45] J. Koepsell, J. Vijayan, P. Sompet, F. Grusdt, T. A. Hilker, E. Demler, G. Salomon, I. Bloch, and C. Gross, Imaging magnetic polarons in the doped fermi-hubbard model, Nature (London) **572**, 358 (2019).

[46] F. Grusdt, M. Kánasz-Nagy, A. Bohrdt, C. S. Chiu, G. Ji, M. Greiner, D. Greif, and E. Demler, Parton Theory of Magnetic Polarons: Mesonic Resonances and Signatures in Dynamics, Phys. Rev. X **8**, 011046 (2018).

[47] See Supplemental Material at http://link.aps.org/supplemental/10.1103/PhysRevLett.127.197004 for details of our time-dependent DMRG simulations, which includes Refs. [48–55].

[48] S. Paeckel, T. Köhler, A. Swoboda, S. R. Manmana, U. Schollwöck, and C. Hubig, Time-evolution methods for matrix-product states, Ann. Phys. (Amsterdam) **411**, 167998 (2019).

[49] J. A. Kjäll, M. P. Zaletel, R. S. K. Mong, J. H. Bardarson, and F. Pollmann, Phase diagram of the anisotropic spin-2 xxz model: Infinite-system density matrix renormalization group study, Phys. Rev. B **87**, 235106 (2013).

[50] M. P. Zaletel, R. S. K. Mong, C. Karrasch, J. E. Moore, and F. Pollmann, Time-evolving a matrix product state with long-ranged interactions, Phys. Rev. B **91**, 165112 (2015).

[51] U. Schollwöck, The density-matrix renormalization group in the age of matrix product states, Ann. Phys. (Amsterdam) **326**, 96 (2011).

[52] J. Hauschild and F. Pollmann, Efficient numerical simulations with Tensor Networks: Tensor Network Python (TeNPy), SciPost Phys. Lect. Notes **5** (2018).

[53] J. Hauschild, R. Mong, F. Pollmann, M. Schulz, L. Schoonderwoert, J. Unfried, Y. Tzeng, and M. Zaletel, The code is available online at https://github.com/tenpy/tenpy/, the documentation can be found at https://tenpy.github.com/ (2018).

[54] A. Auerbach, *Interacting Electrons and Quantum Magnetism* (Springer, Berlin, 1998).

[55] R. Verresen, F. Pollmann, and R. Moessner, Strong quantum interactions prevent quasiparticle decay Nat. Phys. **15**, 750 (2019).

[56] T. P. Devereaux, A. Virosztek, and A. Zawadowski, Charge transfer fluctuation, d-wave superconductivity, and the B_{1g} Raman phonon in cuprates, Phys. Rev. B **51**, 505 (1995).

[57] I. Bloch, J. Dalibard, and W. Zwerger, Many-body physics with ultracold gases, Rev. Mod. Phys. **80**, 885 (2008).

[58] R. B. Laughlin, Evidence for Quasiparticle Decay in Photoemission from Underdoped Cuprates, Phys. Rev. Lett. **79**, 1726 (1997).

[59] L. W. Cheuk, M. A. Nichols, K. R. Lawrence, M. Okan, H. Zhang, E. Khatami, N. Trivedi, T. Paiva, M. Rigol, and M. W. Zwierlein, Observation of spatial charge and spin correlations in the 2d fermi-hubbard model, Science **353**, 1260 (2016).

[60] A. Mazurenko, C. S. Chiu, G. Ji, M. F. Parsons, M. Kanasz-Nagy, R. Schmidt, F. Grusdt, E. Demler, D. Greif, and M. Greiner, A cold-atom fermi-hubbard antiferromagnet, Nature (London) **545**, 462 (2017).

[61] F. Grusdt and L. Pollet, $\mathbb{Z}_2$ Parton Phases in the Mixed-Dimensional $t - J_z$ Model, Phys. Rev. Lett. **125**, 256401 (2020).

[62] J. L. Tallon and J. W. Loram, The doping dependence of T^*—what is the real high-T_c phase diagram? Physica (Amsterdam) **349C**, 53 (2001).

[63] J. Koepsell, D. Bourgund, P. Sompet, S. Hirthe, A. Bohrdt, Y. Wang, F. Grusdt, E. Demler, G. Salomon, C. Gross, and I. Bloch, Microscopic evolution of doped mott insulators from polaronic metal to fermi liquid, Science **374**, 82 (2021).